N72-27723

NASA TECHNICAL MEMORANDUM

NASA TM X-68089

NASA TM X-68089

GAS - CORE REACTOR POWER TRANSIENT ANALYSIS

by Albert F. Kascak
Lewis Research Center
Cleveland, Ohio

TECHNICAL PAPER proposed for presentation at
American Nuclear Society Meeting
Las Vegas, Nevada, June 18-22, 1972

GAS - CORE REACTOR POWER TRANSIENT ANALYSIS

by Albert F. Kascak

Lewis Research Center
National Aeronautics and Space Administration
Cleveland, Ohio

SUMMARY

The gas core reactor is a proposed device which features high temperatures. As such, it has applications in high specific impulse space missions, and possibly in low thermal pollution MHD power plants. In this concept the nuclear fuel is a ball of uranium plasma radiating thermal photons as opposed to gamma rays. This thermal energy is picked up before it reaches the solid cavity liner by an inflowing seeded propellant stream and convected out through a rocket nozzle. A "wall-burn-out" condition will exist if there is not enough flow of propellant to convect the energy back into the cavity. Any real reactor must therefore operate with a certain amount of excess propellant flow. Due to the thermal inertia of the flowing propellant, the reactor can undergo power transients in excess of the steady-state wall burn out power for short periods of time. The objective of this study was to determine how long the wall burn out power could be exceeded without "burning out" the cavity liner.

The model used in the heat-transfer calculation was one-dimensional, and thermal radiation was assumed to be a diffusion process. The energy equation was linearized about the steady state solution, and was solved (with a step increase in power) by using Laplace transformations. Two reactor situations were analyzed; a high power (7400 MW) rocket propulsion reactor, and a low power (3.6 MW) cavity test reactor.

This study showed that the wall burn out time varies as the inverse of the percent increase in reactor power above cavity liner steady state burn out power. When wall burnout power is exceeded by only a few precent, the time to wall burnout is of the order of seconds for the high power reactor and 10's of seconds for the low power reactor. If the wall burnout power is ex-

ceeded by about 10 percent, the wall burnout time is of the order of 0.1 seconds for the high power reactor and seconds for the low power reactor.

INTRODUCTION

The gas-core reactor concept is shown in figure 1. In this concept, the nuclear fuel is a ball of uranium plasma radiating thermal photons as opposed to gamma rays. This thermal energy is picked up before it reaches the solid cavity liner by an inflowing hydrogen stream (propellant) which is seeded with sub-micron size, depleted uranium particles. (The sub-micron particles are used to increase the opacity of the hydrogen at low temperatures.) The propellant first transpirationally cools the cavity liner and then convects the thermal energy out the nozzle of the reactor, (Ref. 1). This type of reactor has application in high specific impulse (5000 s) and moderate thrust (50,000 lb) space missions, (Ref. 2); and in low thermal pollution MHD powerplants, (Ref. 3). Recently a small scale, "test reactor" modification of the gas-core reactor has became of interest, (Ref. 4). It consists of a gas-core cavity imbedded within a solid core "driver" reactor. The purpose of this reactor would be to provide a relatively small size cavity to test gas-core reactor concepts.

In steady state the gas core reactor heat transfer is a balance between radial outward diffusion of thermal photons (heat) and the radial inward convection of the propellant (coolant). A "wall-burnout" condition exists if there is not enough flow of propellant to stop the thermal photons before they reach the cavity liner, Ref. 1. Any real reactor will have some degree of fluctuation about a nominal operating power, and must therefore operate below the wall-burnout power. The farther the reactor must operate below the wall burnout level, the less useful the reactor; therefore, the choice of a nominal reactor operating power becomes a compromise between safety and performance. If the reactor is operating below wall-burnout power level, there can be power transients in excess of the wall burnout power, at least

for short periods of time. This is due to the "thermal inertia" of the hydrogen propellant. The objective of this study was to determine how long the wall burnout power could be exceeded without "burning out" the cavity liner. This time is useful as a guide for estimating the required reaction times of control systems for gas core reactors.

The model used in the heat-transfer calculation was one-dimensional, and thermal radiation transport was assumed to be a diffusion process. The energy equation was linearized about the steady state solution and was solved (with a step increase in power) by using Laplace transformations. The properties of the gases and seed materials used were taken from Ref. 5-10.

SYMBOLS

A	arbitrary integration constant
α_R	Rosseland Mean Absorption Coefficient, m^{-1}
B	arbitrary integration constant
C_p	specific heat at constant pressure, J/(kg-k)
F	defined function of S
f	inverse of F
h	enthalpy, J/kg
K	thermal conductivity, w/m
$\mathcal{L}$	Laplace transform operator
n	sum index
q	heat flux, w/m^2
S	Laplace transform variable
T	temperature, K
t	time, sec
u	unit step function
v	velocity, m/s

x	length from fuel toward wall, m
Y	Laplace transform of change in enthalpy
y	integral transformation of x
Z	exponential transformation of Z
Δ	change from steady state operator
ρ	density, kg/m^3
σ	Stefan-Boltzman constant, 5.6697×10^{-8} $W/(M^2-K^4)$
θ	nondimensional time

Subscripts

mol	molecular
o	evaluated at steady state
∞	evaluated at large distance from origin

ANALYSIS

The model used for the heat-transfer calculation is shown in Fig. 2. The propellant flow enters at a relatively large distance from the origin with a temperature, T_∞. It then flows towards the origin. The positive heat flux from the uranium plasma is applied at the origin. The time dependent energy equation is written as:

$$\rho \frac{\partial h}{\partial t} - \rho v \frac{\partial h}{\partial x} = - \frac{\partial}{\partial x} q$$

For a diffusion process, the heat flux is given by:

$$q = -K \frac{\partial T}{\partial x} = - \frac{K}{C_p} \frac{\partial h}{\partial x}$$

where

$$K = \frac{16\sigma T^3}{3\mathcal{Q}_R} + K_{mol}$$

All the properties are functions of enthalpy alone, and if the enthalpy changes with time:

$$h = h_o + \Delta h$$

$$\rho \approx \rho_o + \rho_o' \, \Delta h$$

$$K \approx K_o + K_o' \, \Delta h$$

The heat flux becomes:

$$q = q_o + \Delta q$$

where

$$q_o = - \frac{K_o}{C_{p_o}} \frac{\partial h_o}{\partial x}$$

and

$$\Delta q \approx - \frac{K_o}{C_{p_o}} \frac{\partial \, \Delta h}{\partial x}$$

The energy equation becomes:

$$\rho_o \frac{\partial \, \Delta h}{\partial t} - (\rho v)_o \frac{\partial \, \Delta h}{\partial x} = + \frac{\partial}{\partial x} \left(\frac{K_o}{C_{p_o}} \frac{\partial \, \Delta h}{\partial x} \right)$$

If we define:

$$y \equiv (\rho v)_o \int_0^x \frac{C_{p_o}}{K_o} dx$$

then

$$\frac{\partial}{\partial y} = \frac{dx}{dy} \frac{\partial}{\partial x} = \left(\frac{K}{\rho v C_p} \right)_o \frac{\partial}{\partial x}$$

The energy equation can then be written as:

$$\left(\frac{\rho K}{(\rho v)^2 C_p} \right)_o \frac{\partial \Delta h}{\partial t} = \frac{\partial}{\partial y} \left\{ \frac{\partial}{\partial y} \Delta h + \Delta h \right\}$$

If the variables are transformed to

$$Z = e^{-y}$$

$$\theta = \left(\frac{(\rho v)^2 C_p}{\rho K} \right)_o Z^2 t$$

then the energy equation becomes

$$\frac{\partial}{\partial \theta} \Delta h = \frac{\partial^2}{\partial Z^2} \Delta h$$

The initial condition is

$$\Delta h(0, Z) = 0$$

The boundary condition at some large distance from the origin is

$$\Delta h(\theta, 0) = 0$$

The boundary condition at the origin is

$$\frac{\partial}{\partial Z} \Delta h(\theta, 1) = \left(\frac{\Delta q}{\rho v}\right)\Bigg|_{(0,1)} u(\theta)$$

If θ is Laplace transformed into S and

$$Y \equiv \mathcal{L}(\Delta h)$$

then using the initial condition the energy equation becomes

$$SY(S, Z) = \frac{\partial^2}{\partial Z^2} Y(S, Z)$$

This equation can be integrated and becomes

$$Y(S, Z) = A(S)e^{+\sqrt{S}\, Z} + B(S)e^{-\sqrt{S}\, Z}$$

Applying the boundary condition at large distances from the origin

$$Y(S, 0) = A + B = 0$$

Applying the boundary condition at the origin

$$\frac{\partial}{\partial Z} Y(S, 1) = \left(\frac{\Delta q}{\rho v}\right)\Bigg|_{(0,1)} \frac{1}{S}$$

and solving for A and B; the solution becomes:

$$Y(S, Z) = \left(\frac{\Delta q}{\rho v}\right)\Bigg|_{(0,1)} \frac{(e^{+\sqrt{S}\,Z} - e^{-\sqrt{S}\,Z})}{S^{3/2}(e^{+\sqrt{S}} + e^{-\sqrt{S}})}$$

The denominator can be expanded in a Taylor series:

$$Y(S, Z) = \left(\frac{\Delta q}{\rho v}\right)\Bigg|_{(0,1)} \sum_{n=0}^{\infty} (-1)^n S^{-3/2} \left\{e^{+(Z-1-2n)\sqrt{S}} - e^{-(Z+1+2n)\sqrt{S}}\right\}$$

If the following function is defined as:

$$F(S, K) = S^{-3/2}\, e^{-K\sqrt{S}} \qquad K \geq 0$$

then its inverse is:

$$f(\theta, K) = 2\sqrt{\frac{\theta}{\pi}}\, e^{-(K^2/4\theta)} - K \operatorname{erfc} \frac{K}{2\sqrt{\theta}}$$

where erfc is the complementary error function. The change in enthalpy in response to a step increase in heat flux at the origin at time zero then becomes

$$\Delta h(\theta, Z) = \left(\frac{\Delta q}{\rho v}\right)\Bigg|_{(0,1)} \sum_{n=0}^{\infty} (-1)^n \left\{f(\theta, 2n + 1 - Z) - f(\theta, 2n + 1 + Z)\right\}$$

The change in enthalpy in response to a pulse increase of heat flux at the origin and applied from time zero to time one then becomes

$$\Delta h(\theta, Z) = \left(\frac{\Delta q}{\rho v}\right)\Bigg|_{(0,1)} \sum_{n=0}^{\infty} (-1)^n \Big\{ f(\theta, 2n + 1 - Z) - f(\theta, 2n + 1 + Z)$$

$$- u(\theta - \theta_1)\Big[f(\theta - \theta_1, 2n + 1 - Z) - f(\theta - \theta_1, 2n + 1 + Z)\Big]\Big\}$$

The change in enthalpy in response to a delta function increase of heat flux at the origin is

$$\Delta h(\theta, Z) = \left(\frac{\Delta q\ \Delta\theta}{\rho v}\right)\Bigg|_{(0,1)} \sum_{n=0}^{\infty} \frac{(-1)^n}{\pi\theta} \left\{ e^{-(2n+1-Z)^2/4\theta} - e^{-(2n+1+Z)^2/4\theta} \right\}$$

The change in enthalpy in response to a arbitrary function increase of heat flux at the origin is

$$\Delta h(\theta, Z) = \int_0^{\theta} \left(\frac{\Delta q}{\rho v}\right)\Bigg|_{(\theta', 1)} \sum_{n=0}^{\infty} \frac{(-1)^n}{\pi(\theta - \theta')} \left\{ e^{-(2n+1-Z)^2/4(\theta - \theta')} \right.$$

$$\left. - e^{-(2n+1+Z)^2/4(\theta - \theta')} \right\} d\theta'$$

If it is assumed that the initial condition is steady state; then

$$-(\rho v)_o \frac{\partial h_o}{\partial x} = \frac{\partial}{\partial x}\left(\frac{K_o}{C_{p_o}} \frac{\partial h_o}{\partial x}\right)$$

Integrating from x to ∞ gives

$$(\rho v_o)(h_o - h_\infty) = - \frac{K_o}{C_{p_o}} \frac{\partial h_o}{\partial x} = q_o$$

Integrating from 0 to x gives

$$x = \frac{1}{(\rho v)_o} \int_{h_o(0)}^{h_o(x)} \frac{K\, dh}{C_p(h - h_\infty)}$$

where

$$h_o(0) = \frac{q_o(0)}{(\rho v)_o} + h_\infty$$

The calculational method used was as follows. First, the initial steady state temperature profile was calculated. Next, the perturbation about this temperature profile was calculated at the next increment in time. Third, the new properties at this "perturbed" temperature were calculated. This process was repeated until the final time was reached, along with the corresponding temperature profile and associated properties.

DISCUSSION OF RESULTS

A cross section of the gas-core reactor is shown on Fig. 1. The propellant flows through the cavity wall, transpirationally cooling the wall. Then the propellant flows from the wall toward the fissioning uranium plasma convecting the radiant heat that it absorbs back toward the fuel and finally out of the reactor. This process was modeled with a one-dimensional, time dependent perturbation method. The reactor described in Ref. 1; with a maximum power of 7400 MW and a modification of the reactor described in Ref. 4 with a maximum power of 3.6 MW was analyzed. The objective of this study was to determine how long the maximum reactor power could be exceeded without burning out the cavity liner.

Figure 3 illustrates some of the complexity of the problem. It shows the "Rosseland Mean Absorption Coefficient" versus temperature. At relatively low temperatures, the solid seed is the dominant absorber. As the temperature increases, the solid-seed absorption coefficient decreases because the propellant density decreases - which in turn causes the number of solid particles per unit volume to decrease. At some temperature (~5000 K) the solid seed begins to vaporize, and this causes the absorption coefficient to decrease rather sharply, at least according to current estimates. In the temperature region between 7000-10 000 K, the absorption is due mainly to seed vapor, which in this case is represented by depleted uranium vapor properties. At temperatures above 10 000 K, the absorption is due mainly to the hydrogen propellant itself.

Figure 4 shows results of some reactor power transient calculations. Typical radial temperature profiles in the region between the fuel and the cavity liner at specified times after initiation of a step power increase are plotted for the reactors of Refs. 1 and 4. Figure 4-A shows the reactor of Ref. 1. In this reactor the distance between the fuel and the cavity liner is about 0.4 m. About 4.5 kg/s of propellant flows radially inward from the cavity liner. The wall burn out power for this reactor is 7400 MW, and the initial reactor power is 9.1 percent below the steady state wall burn out power. Figure 4-B shows a reactor similar to the one in Ref. 4. In this reactor, the distance between the fuel and the cavity liner is about 0.11 m and about 0.1 kg/s of propellant flows in through the cavity liner. The wall burn out power for this reactor is 3.6 MW; the initial reactor power is 9.1 percent below wall burn out power.

In Fig. 4-A the reactor of Ref. 1 is assumed to be operating at a steady state power that is 9.1 percent below the cavity liner burn-out power. At time zero, the reactor power is given a step increase of 15 percent and is now operating at 105 percent of wall burn out power. Typical radial temperature profiles in the region between the fuel and the cavity liner are shown at times of 0, 0.1, 0.2, 0.3, and ∞ sec. At about 0.4 seconds into the transient period, the cavity liner burn out condition is reached. The transient

temperature profiles are similar to the steady state profiles. A temperature "front" seems to propagate towards the cavity wall with diminishing velocity during the power transient.

In Fig. 4-B the reactor similar to Ref. 4 is assumed to be operating at a steady state power that is 9.1 percent below the cavity liner burn-out power. At time zero, the reactor power is given a step increase of 15 percent and is now operating at 105 percent of wall burn out power. Typical radial temperature profiles in the region between the fuel and the cavity liner are shown at times of 0, 1, 2, 3, 4, 5, and ∞ sec. At about 5 seconds into the transient period, the cavity liner burn-out condition is reached. The transient temperature profiles are again similar to the steady state profiles.

The burn out time is of course a function of the degree to which the transient power exceeds the wall burn-out power. Figure 5 shows the time to wall burn out versus the percent power increase above initial steady state. The initial steady state power is either 9.1 or 16.7 percent below wall burn out. That is an increase of initial steady state power of either 10 or 20 percent will result in wall burn out at infinite time. Figure 5-A shows the cases for the reactor of Ref. 1, and Fig. 5-B shows the case for the reactor similar to Ref. 4.

The time to wall burn out is longer for less severe power transients. For example a 25 percent increase in initial steady state power results in wall burn out at 0.15 sec for the high power reactor operating at 9.1 percent of wall burnout power; while for the same reactor and transient operating at 16.7 percent of wall burn out power results in wall burn out at something greater than 1 sec. The same thing is seen for the low power reactor except the time to wall burn out is about ten times as long. The conclusion that can be reached is that when wall burnout power is exceeded by only a few percent the time to wall burn out can be of the order of seconds for the high power reactor and 10 of seconds for the low power reactor. If the wall burnout power is exceeded by greater then 10 percent, the wall burn out time is the order of 0.1 second for the high power reactor and seconds for the low power reactor. The low power reactor can probably be contiuously controlled with

power pulse in excess of wall burnout, while the high power reactor can not. The high power reactor will have to be designed not to exceed 110 percent of wall burnout. If it does a scram will have to be initialed and the reactor will have to shut down in tenths of seconds.

CONCLUSIONS

The temperature response of a gas-core reactor was analyzed when subjected to a power transient. The objective of this study was to determine how long the maximum steady state reactor power could be exceeded without burning out the cavity liner. The relatively large magnitudes of reactor power transients considered here would probably be precursors of a reactor scram, rather than normal reactor fluctuations.

The wall burn-out time varies as the inverse of the percent increase in reactor power above cavity liner steady state burnout power. The transient temperature profiles appear to be similar to steady state temperature profiles. When wall burnout power is exceeded by only a few percent, the time to wall burnout can be of the order of seconds for the high power reactor and 10's of seconds for the low power reactor. If the wall burnout power is exceeded by about 10 percent, the wall burnout time is of the order of 0.1 seconds for the high power reactor and seconds for the low power reactor.

REFERENCES

1. Kascak, A. F.: Nozzle and Cavity Wall Cooling Limitations on Specific Impulse of a Gas-Core Nuclear Rocket. Second Symposium on Uranium Plasma, Atlanta, Georgia, November 15-17, 1971, NASA TM X-67923.

2. Ragsdale, R. B. and Willis, E. A.: Gas-Core Rocket Reactors - A New Look. Paper No. 71-641, June 1971, AIAA, Salt Lake City, Utah. NASA TM X-67823.

3. Williams, J. R.: An Evaluation of Gas-Core Reactors with MHD Conversion for Clean, Economical Power Generation. Second Symposium on Uranium Plasma, AIAA, Atlanta, Georgia, November 15-17, 1971.

4. Hyland, R. E.: A Mini-Cavity Reactor for Low Thrust High Specific Impulse Propulsion. Spacecraft and Rockets, March 15, 1972.

5. Parks, D. E., Lane, G., Steward, J. C., and Peyton, S.: Optical Constants of Uranium Plasma. GA-8244, February 1968, Gulf General Atomic, San Diego, California.

6. Pattoret, A., Smoes, S., and Drowart, J.: Thermodynamic Studies of Mass Spectrometry, Thermodynamic Study of the Uranium-Oxygen System by Mass Spectrometry: The Heat of Sublimation of Uranium. EUR-2458.f, 1965, Brussels University, Belgium.

7. Patch, R. W.: Interim Absorption Coefficients and Opacities for Hydrogen Plasma at High Pressure. NASA TM X-1902, October 1969.

8. Patch, R. W.: Thermodynamic Properties and Theoretical Rocket Performance of Hydrogen to $100,000^{\circ}$ K and 1.01325×10^{8} N/m^{2}. Proposed NASA Technical Note.

9. Grier, N. T.: Calculation of Transport Properties and Heat-Transfer Parameters of Dissociating Hydrogen. NASA TN D-1406, October 1962.

10. Grier, N. T.: Calculation of Transport Properties of Ionizing Atomic Hydrogen. NASA TN D-3186, April 1966.

3. Williams, J. R.: An Evaluation of Gas-Core Reactors with MHD Conversion for Clean, Economical Power Generation. Second Symposium on Uranium Plasma, AIAA, Atlanta, Georgia, November 15-17, 1971.

4. Hyland, R. E.: A Mini-Cavity Reactor for Low Thrust High Specific Impulse Propulsion. Spacecraft and Rockets, March 15, 1972.

5. Parks, D. E., Lane, G., Steward, J. C., and Peyton, S.: Optical Constants of Uranium Plasma. GA-8244, February 1968, Gulf General Atomic, San Diego, California.

6. Pattoret, A., Smoes, S., and Drowart, J.: Thermodynamic Studies of Mass Spectrometry, Thermodynamic Study of the Uranium-Oxygen System by Mass Spectrometry: The Heat of Sublimation of Uranium. EUR-2458.f, 1965, Brussels University, Belgium.

7. Patch, R. W.: Interim Absorption Coefficients and Opacities for Hydrogen Plasma at High Pressure. NASA TM X-1902, October 1969.

8. Patch, R. W.: Thermodynamic Properties and Theoretical Rocket Performance of Hydrogen to $100,000^{\circ}$ K and 1.01325×10^{8} N/m^{2}. Proposed NASA Technical Note.

9. Grier, N. T.: Calculation of Transport Properties and Heat-Transfer Parameters of Dissociating Hydrogen. NASA TN D-1406, October 1962.

10. Grier, N. T.: Calculation of Transport Properties of Ionizing Atomic Hydrogen. NASA TN D-3186, April 1966.

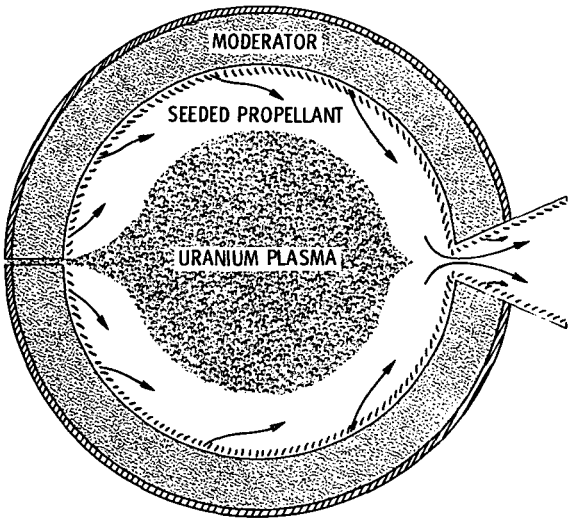

Figure 1. - Gas core reactor.

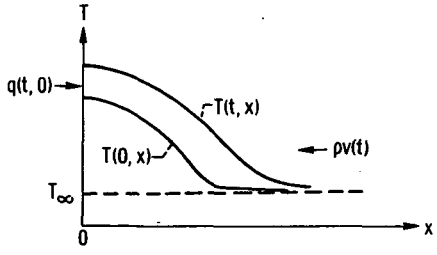

Figure 2. - Heat transfer model.

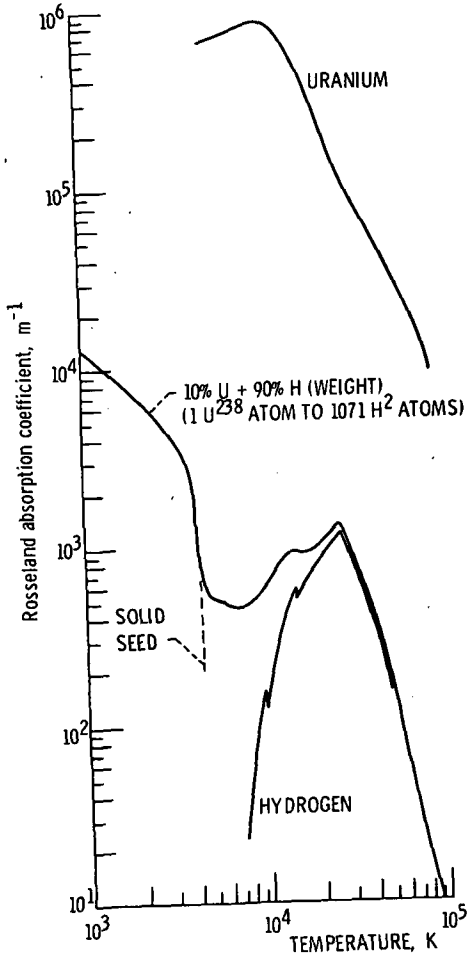

Figure 3. - Rosseland absorption coefficient versus temperature at 1000 atmosphere, 1.01×10^{-8} N/m^2.

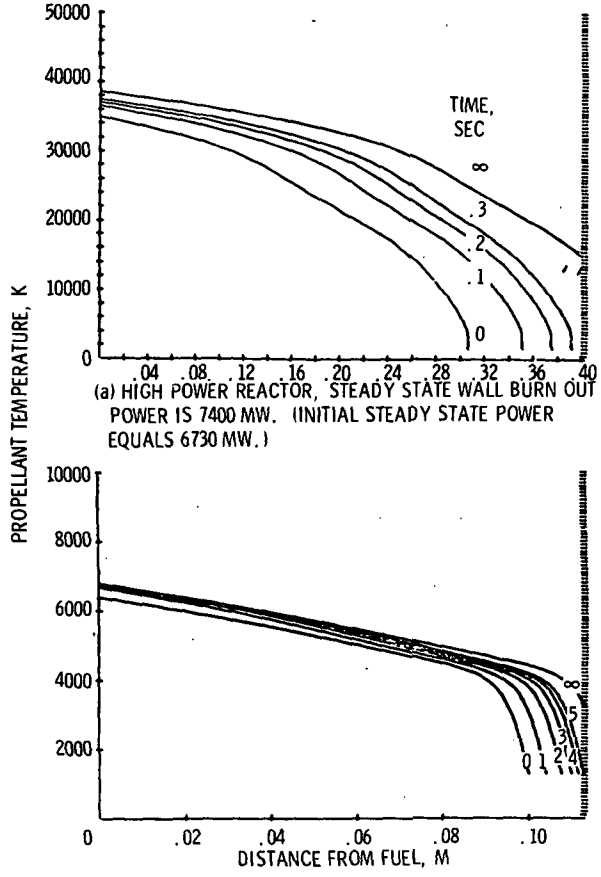

(a) HIGH POWER REACTOR, STEADY STATE WALL BURN OUT POWER IS 7400 MW. (INITIAL STEADY STATE POWER EQUALS 6730 MW.)

(b) LOW POWER REACTOR, STEADY STATE WALL BURN OUT POWER IS 3.6 MW. (INITIAL STEADY STATE POWER EQUALS 3.27 MW.)

Figure 4. - Typical radial temperature profile in the region between the fuel and the cavity liner at specified times after initiation of a 15 percent step power increase.

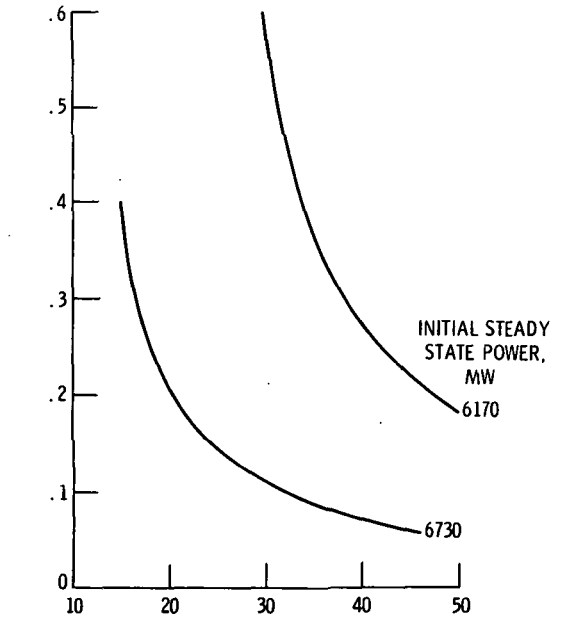

(a) HIGH POWER REACTOR, (STEADY STATE WALL BURN OUT POWER EQUALS 7400 MW).

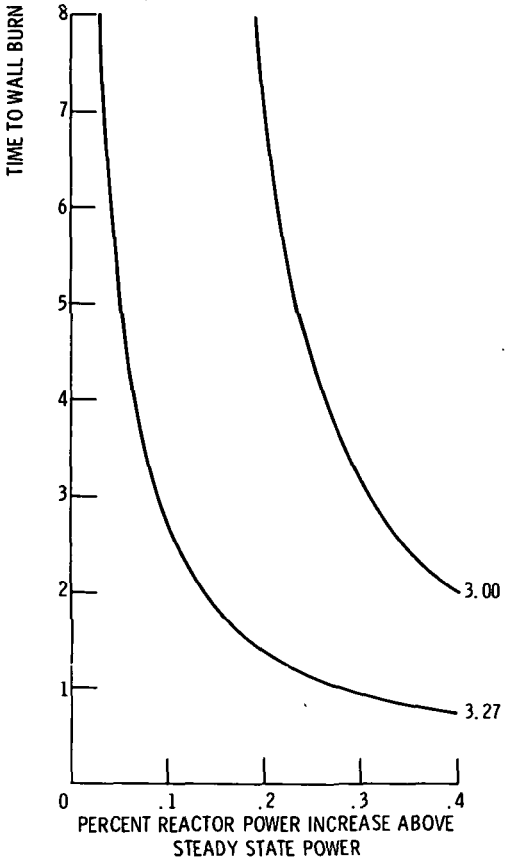

(b) LOW POWER REACTOR (STEADY STATE WALL BURN OUT POWER EQUALS 3.6 MW).

Figure 5. - Time to cavity wall burnout during power surge.